

# Four-year polymer biocompatibility and vascular healing profile of a novel ultrahigh molecular weight amorphous PLLA bioresorbable vascular scaffold: an OCT study in healthy porcine coronary arteries



Torsten P. Vahl<sup>1,2</sup>, MD; Pawel Gasior<sup>1,3</sup>, MD, PhD; Carlos A. Gongora<sup>1</sup>, MD; Kamal Ramzipoor<sup>4</sup>, BS, ME; Chang Lee<sup>4</sup>, BS, MS, ME; Yanping Cheng<sup>1</sup>, MD; Jenn McGregor<sup>1</sup>, BS; Masahiko Shibuya<sup>1</sup>, MD; Edward A. Estrada<sup>4</sup>, BS, ME; Gerard B. Conditt<sup>1</sup>, RCIS; Greg L. Kaluza<sup>1</sup>, MD, PhD; Juan F. Granada<sup>1\*</sup>, MD

1. CRF-Skirball Center for Innovation, New York, NY, USA; 2. Center for Interventional Vascular Therapy, Columbia University Medical Center, New York Presbyterian Hospital, New York, NY, USA; 3. Medical University of Silesia, 3rd Department of Cardiology, Medical University of Silesia, Katowice, Poland; 4. Amaranth Medical, Inc., Mountain View, CA, USA

## KEYWORDS

- bare metal stent
- bioresorbable scaffolds
- in-stent restenosis
- optical coherence tomography
- preclinical research

## Abstract

**Aims:** The vascular healing profile of polymers used in bioresorbable vascular scaffolds (BRS) has not been fully characterised in the absence of antiproliferative drugs. In this study, we aimed to compare the polymer biocompatibility profile and vascular healing response of a novel ultrahigh molecular weight amorphous PLLA BRS (FORTITUDE<sup>®</sup>; Amaranth Medical, Mountain View, CA, USA) against bare metal stent (BMS) controls in porcine coronary arteries.

**Methods and results:** Following device implantation, optical coherence tomography (OCT) evaluation was performed at 0 and 28 days, and at one, two, three and four years. A second group of animals underwent histomorphometric evaluation at 28 and 90 days. At four years, both lumen (BRS 13.19±1.50 mm<sup>2</sup> vs. BMS 7.69±2.41 mm<sup>2</sup>) and scaffold areas (BRS 15.62±1.95 mm<sup>2</sup> vs. BMS 8.65±2.37 mm<sup>2</sup>) were significantly greater for BRS than BMS controls. The degree of neointimal proliferation was comparable between groups. Histology up to 90 days showed comparable healing and inflammation profiles for both devices.

**Conclusions:** At four years, the novel PLLA BRS elicited a vascular healing response comparable to BMS in healthy pigs. Expansive vascular remodelling was evident only in the BRS group, a biological phenomenon that appears to be independent of the presence of antiproliferative drugs.

\*Corresponding author: CRF - Skirball Center for Innovation, 8 Corporate Drive, Orangeburg, NY 10962, USA.  
E-mail: jgranada@crf.org

## Abbreviations

<b>BMS</b>	bare metal stent(s)
<b>BRS</b>	bioresorbable scaffold(s)
<b>CAD</b>	coronary artery disease
<b>DAPT</b>	dual antiplatelet therapy
<b>DES</b>	drug-eluting stent(s)
<b>LA</b>	lumen area
<b>MW</b>	molecular weight
<b>NIT</b>	neointimal thickness
<b>OCT</b>	optical coherence tomography
<b>%AS</b>	percentage area stenosis
<b>PLLA</b>	poly-L-lactic acid
<b>SA</b>	inner scaffold area or stent area

## Introduction

Bioresorbable vascular scaffolds (BRS) are emerging as an alternative therapeutic approach to metallic drug-eluting stents (DES) due to their ability to support the arterial segment mechanically in the early phases post intervention, followed by progressive dismantling and absorption of the scaffold over time<sup>1,2</sup>. First-generation BRS rely on poly-L-lactic acid (PLLA) crystallinity to achieve mechanical properties comparable to metallic stents, but they are limited by their inability to overexpand beyond pre-specified limits and to maintain structural integrity when exposed to high loading conditions over time<sup>3</sup>. Novel ultrahigh molecular weight amorphous PLLA polymers display superior mechanical properties and promise to improve some of the technical limitations of current-generation BRS technologies.

First-generation BRS using crystalline PLLA analogues have been extensively studied in the experimental and clinical setting<sup>4-8</sup>. Several studies have shown that these devices induce progressive expansive remodelling and have a vascular healing profile comparable to metallic DES in animals<sup>9</sup> and humans<sup>10-12</sup>. However, there is limited information on the impact of polymer degradation on vascular healing and remodelling in the absence of antiproliferative drugs. The aim of this study was to test the *in vivo* long-term biomechanical properties and vascular healing profile of an ultrahigh molecular weight amorphous PLLA BRS (FORTITUDE<sup>®</sup>; Amaranth Medical, Mountain View, CA, USA) against a bare metal stent (BMS) in healthy porcine coronary arteries. The use of a non-drug-eluting BRS allowed us to assess the independent impact of the polymer on the arterial wall response without any interference from antiproliferative drugs. Also, the presence of the PLLA-based scaffold polymer exceeds the duration of sirolimus elution in drug-eluting platforms, and therefore the biocompatibility of the polymer remains an important scaffold characteristic.

## Methods

### DEVICE DESCRIPTION

The first-generation FORTITUDE BRS is manufactured using an ultrahigh molecular weight bioresorbable PLLA polymer with a strut thickness of 150 microns. Three platinum radiopaque markers are incorporated at both ends to improve angiographic

visualisation. The clinically available BRS is coated with a matrix consisting of 1:1 polymer:drug ratio of sirolimus plus poly(D-lactide) polymer and has a drug dosing of ~96 µg/cm<sup>2</sup>. The core BRS technology involves a proprietary process of very high molecular weight (MW) polymer synthesis and processing, designed to achieve a balance between strength, flexibility and high resistance to fracture. Tube manufacturing is achieved by a proprietary multilayer deposition process. The biomechanical properties of the polymer are fully preserved throughout the manufacturing cycle with negligible reduction of MW and no alteration of thermal properties from PLLA tubing fabrication to the final sterile device. In the current study, the non-drug-eluting BRS version was used and compared to an FDA-approved, commercially available thin-strut (96 microns) bare metal stent (BMS) (Liberté<sup>®</sup>; Boston Scientific, Marlborough, MA, USA).

### IN VITRO SCAFFOLD DEGRADATION AND RADIAL FORCE

The degradation profile and radial strength of the BRS were assessed *in vitro* over a period of 18 months. The expanded BRS were placed in a shaker containing sterile phosphate buffered saline solution. The devices were incubated at a constant temperature of 37° Celsius and a pH of 7.4±0.2 throughout the study. The MW of the scaffold was measured at each time point using gel permeation chromatography. The corresponding radial force of the samples was measured at the same time points using a J-Crimp<sup>™</sup> radial force testing system (Blockwise Engineering, Tempe, AZ, USA).

### IN VIVO POLYMER BIOCOMPATIBILITY AND HEALING STUDIES

The Institutional Animal Care and Use Committee approved this study, and all animals received care in accordance with the Guide to Care and Use of Laboratory Animals. To evaluate early tissue compatibility and the healing of the FORTITUDE BRS in direct comparison to BMS, we performed OCT measurements and histomorphometric analyses of a group of 16 young adult Yucatan minipigs at 28 (group 1A) or 90 days (group 1B). Therefore, 15 BRS and 16 BMS were implanted among all three coronary arteries, and the implant location was determined by the size of the coronary arteries. All BRS and BMS were implanted with an optimal overstretch ratio of 1:1.1. On day 28, OCT and histology were assessed in n=11 BRS and n=10 BMS; in the 90-day animals the same assessment was performed in n=4 BRS and n=6 BMS. A second group of four young adult Yucatan minipigs (group 2A, BRS=6, BMS=4) was used for a long-term study in which serial OCT measurements were performed immediately after implantation, at 28 days, and at one, two, three, and four years. One animal was sacrificed after two years for polymer analysis such that only four BRS and three BRS could be evaluated at three and four years. Because of the relatively small sample size for long-term follow-up, we performed OCT measurements in four additional animals (group 2B) up to four years which had been implanted with a total of seven BRS. These animals received BRS only and had no BMS controls.

The device implantation was performed with a standard percutaneous technique utilising intravenous heparin for anticoagulation.

Dual antiplatelet therapy consisting of oral clopidogrel and aspirin was initiated the day prior to the procedure and maintained throughout the study. Mean vessel diameters were measured by IVUS to guide sizing of the devices. All BRS (sizes 3.3×18 mm and 3.65×18 mm) and BMS (sizes 2.75×20, 3.0×20, 3.5×20 and 4.0×20 mm) were implanted using an overstretch ratio of 1:1.1 in all three coronary arteries. Angiography and OCT were performed immediately after implantation and during all follow-up time points.

### OPTICAL COHERENCE TOMOGRAPHY IMAGING

OCT images were recorded using the C7-XR OCT imaging system (ImageWire™; LightLab Imaging, St. Jude Medical, St. Paul, MN, USA) and analysed using commercial software. OCT analysis involved assessment of cross-sectional images inside the scaffold, and proximal and distal reference segments were defined as ~5 mm from the proximal and distal scaffold edge, respectively. The following parameters were measured after calibration: LA=lumen area, SA=inner scaffold area or stent area, percentage area stenosis (%AS=[1-(LA/SA)])×100, neointimal thickness (NIT), measured as the distance from the inner surface of the stent struts to the luminal border. In order to normalise the lumen changes to the variations in the reference vessel size, patency ratio was calculated as follow-up LA/follow-up reference vessel area, and its changes also evaluated at different time points. The patency ratio was calculated to determine the relationship between the calibre of the stent-treated (or scaffold-treated) vessel region versus the calibre of the reference vessel segments proximal and distal to the treated region.

### HISTOLOGICAL ANALYSIS

An independent pathology laboratory (Alizee Pathology LLC, Thurmont, MD, USA) conducted the histomorphometric analysis. Coronary arteries were prepared and the cross-sectional areas were measured as previously described<sup>11</sup>. The resulting slides were examined via light microscopy. The cross-sectional areas (external elastic lamina, internal elastic lamina and LA) of each section were measured. Degree of vascular injury, presence of vascular inflammation, fibrin deposition, fibrosis, luminal thrombosis and medial hypocellularity were evaluated under the following semi-quantitative score: 0=not present; 1=present, but minimal feature; 2=notable feature, mild; 3=prominent feature, not disrupting tissue architecture and not overwhelming, moderate; 4=overwhelming feature or feature effacing or disrupting tissue architecture, severe. Endothelialisation was evaluated according to the percentage of neointimal endothelial coverage (0 ≤25%, 1=25-50%, 2=50-70%, 3=70-95%, 4 >95%).

### STATISTICAL ANALYSES

Statistical analysis was conducted using SigmaPlot 12 (Systat Software, Inc., San Jose, CA, USA). All values are expressed as mean±standard deviation. Values were compared between groups using non-parametric Mann-Whitney U tests. ANOVA for repeated measures was used for the longitudinal analyses. *Post hoc* analysis with the Holm-Sidak procedure was performed when

the overall analysis of a multiple group comparison was significant. A p-value below 0.05 was considered statistically significant.

## Results

### IN VITRO SCAFFOLD DEGRADATION AND RADIAL FORCE ASSESSMENT

Results from the *in vitro* scaffold degradation and radial force changes over time are shown in **Figure 1**. There was a continued reduction of the MW over time, reaching approximately 50% of the initial MW at eight months and nearly 75% at 12 months. The scaffold continued to degrade over time, and at the last time point (18 months) the reduction in MW had reached more than 85%. Importantly, there was a substantial increase in radial force from time zero to one month, which was sustained at that level for 10 months. After this period, when the MW had decreased to less than 50%, the radial force decreased in a linear fashion up to the 18-month follow-up.

### IN VIVO VESSEL HEALING AND REMODELLING OCT ANALYSIS

Following device implantation, no differences were observed between BRS and BMS in terms of lumen (7.29±0.80 vs. 7.36±1.59 mm<sup>2</sup>, p=ns) or reference areas (7.04±0.4 vs. 7.05±2.10 mm<sup>2</sup>, p=ns). **Figure 2A** illustrates representative OCT images demonstrating the evolution of the BRS integration into the arterial wall and changes in the lumen area over time. At 28 days, the BMS group showed nearly a 28% decrease in lumen area due to neointimal proliferation (**Figure 2B**). Thereafter, the average lumen area increased again towards the baseline value, which was reached at three years. Similarly, the BRS group experienced an early lumen area loss of nearly 31% at 28 days. However, the lumen area returned nearly to baseline as early as one year after implantation, and increased significantly thereafter throughout the four-year follow-up (a twofold increase over baseline at four years, p<0.001) (**Figure 2B**). Importantly, the BRS lumen area increased at a rate matching that observed in the reference segments (**Figure 3A**). In contrast, the lumen area of the

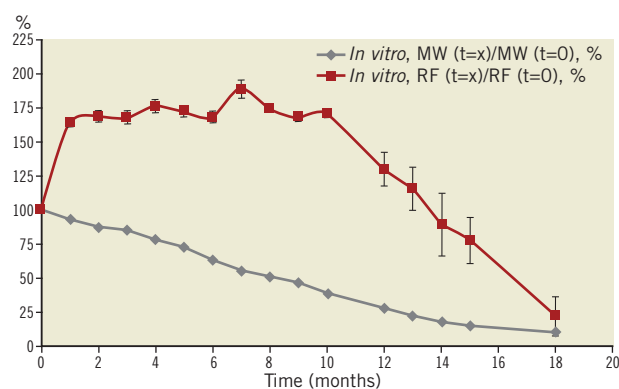


**Figure 1.** *In vitro* degradation and physical properties of the FORTITUDE bioresorbable vascular scaffold (3.0×18 mm). The grey line depicts the reduction in MW over time. The red line indicates the change in radial force (RF) over the course of 18 months.

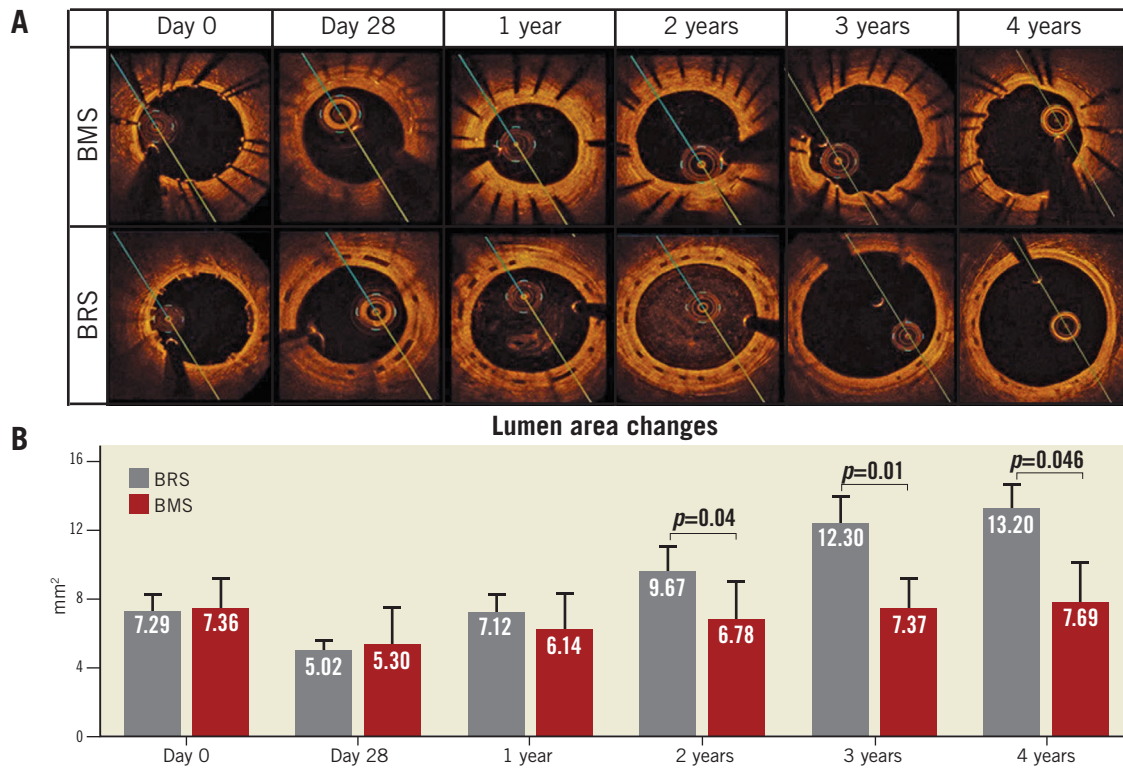


**Figure 2.** Comparison of lumen area changes over time between BMS and BRS. A) Representative images of the longitudinal assessment with OCT are shown for BMS (top panel) and BRS (bottom panel). B) Longitudinal assessment of in-stent lumen area in BRS (grey) and BMS (red) by OCT over the course of four years.

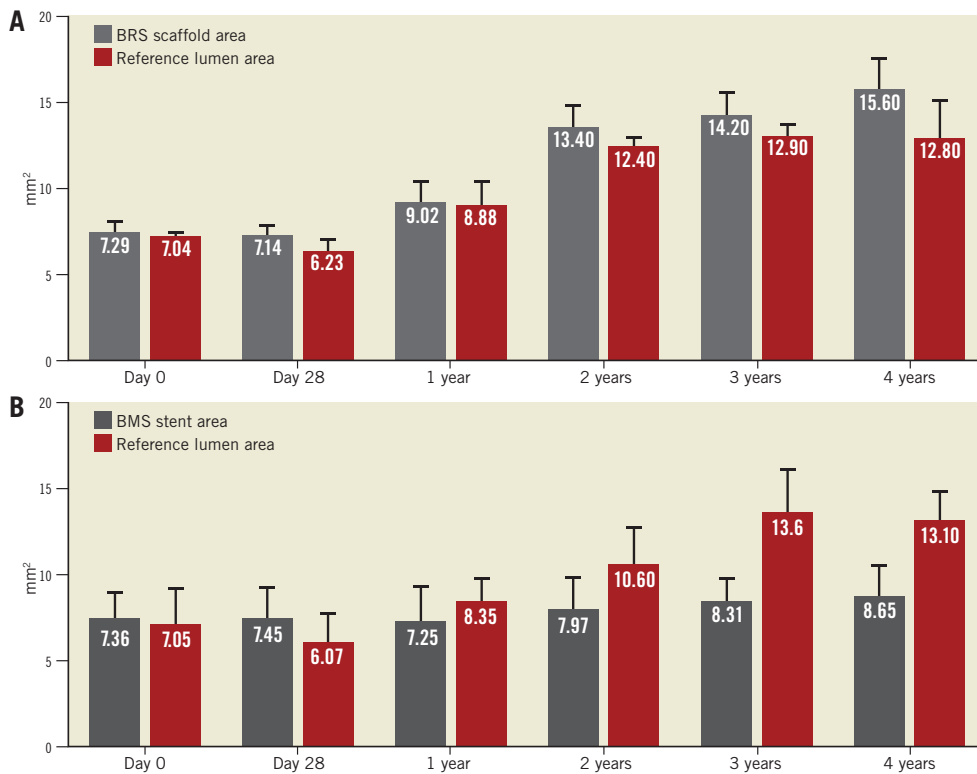


**Figure 3.** Reference lumen area and scaffold/stent evaluation over the course of four years. Comparison of reference area and scaffold/stent area in BRS (A) and BMS (B) by OCT. In BRS, both the reference and the scaffold area increase over time. In contrast, in BMS vessels only the reference area increases but the stent area remains constant.

coronary segments treated with BMS did not expand in concert with the reference segments (**Figure 3B**). NIT and %AS were similar in both groups at all time points; however, the patency ratio increased over time in the BRS group and decreased in the BMS group (**Figure 4**). **Figure 5** demonstrates the changes in animal weight over time in groups 2A and 2B. The long-term BRS results are supported by the data from the longitudinal cohort of animals treated with BRS only (group 2B). The three- and four-year results correspond well with the outcomes in the direct comparison of BRS and BMS (**Figure 6**).

### HISTOLOGICAL EVALUATION OF HEALING

The results obtained by histomorphometry were comparable to those obtained by OCT at 28 and 90 days. As shown in **Table 1**, no significant differences were seen in LA, %AS or NIT between the study groups at 28 or 90 days. **Table 2** shows the histological assessment of biocompatibility and safety variables in BRS and BMS stents at both time points. In addition, there was no evidence of delayed healing or impairment in neointimal maturity between groups. Importantly, the struts of both BRS and BMS were fully endothelialised in the 28- and 90-day specimens (**Figure 7**). A slight amount of residual fibrin was observed in both groups at 28 days that was fully resolved at 90 days. Neointimal scores were very low in both groups at both time points. There was slightly more peri-strut inflammation in the BRS group at 90 days, but it remained in the “low to mild” category.

**Table 1. Histomorphometric analysis at 28 and 90 days.**

	BRS	BMS	p-value
<b>28 days</b>			
EEL area, mm <sup>2</sup>	7.51±0.46	8.93±2.31	0.379
Lumen area, mm <sup>2</sup>	3.81±1.17	5.30±1.55	0.028
IEL area, mm <sup>2</sup>	6.29±0.37	7.62±2.04	0.342
Neointimal area, mm <sup>2</sup>	2.48±1.10	2.32±1.06	0.916
Neointimal thickness, mm	0.33±0.18	0.26±0.11	0.460
% area stenosis	39.64±18.03	30.60±11.06	0.306
<b>90 days</b>			
EEL area, mm <sup>2</sup>	7.50±0.87	8.92±2.65	0.231
Lumen area, mm <sup>2</sup>	3.43±1.08	4.95±2.23	0.195
IEL area, mm <sup>2</sup>	6.03±0.70	7.65±2.32	0.160
Neointimal area, mm <sup>2</sup>	2.67±0.50	2.71±1.90	0.530
Neointimal thickness, mm	0.36±0.09	0.42±0.26	0.652
% area stenosis	44.75±11.32	35.17±17.53	0.392

EEL: external elastic lamina; IEL: internal elastic lamina

### Discussion

The present study assessed the four-year *in vivo* biomechanical behaviour and vascular healing profile of a novel PLLA-based BRS in the absence of antiproliferative drugs. The device was implanted in normal porcine coronary arteries, which we directly compared to a clinically available BMS. Our histological and intravascular imaging analyses demonstrated that the biological behaviour of this

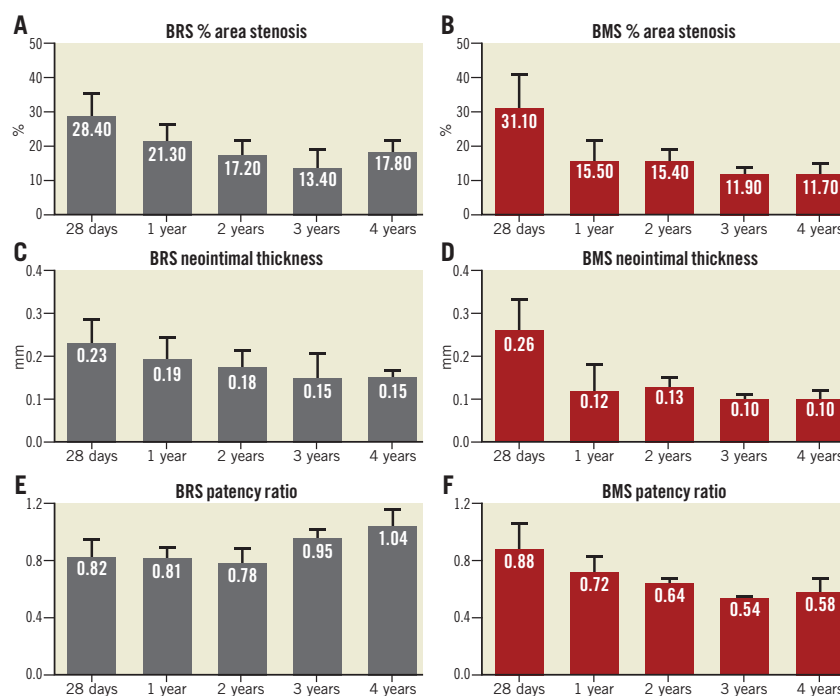


**Figure 4.** Neointimal proliferation evaluation over the course of four years. BRS and BMS groups both demonstrated reduction over time in %AS (A & B) and neointimal thickness (C & D). The patency ratio increased over time in the BRS group and decreased in the BMS group (E & F).



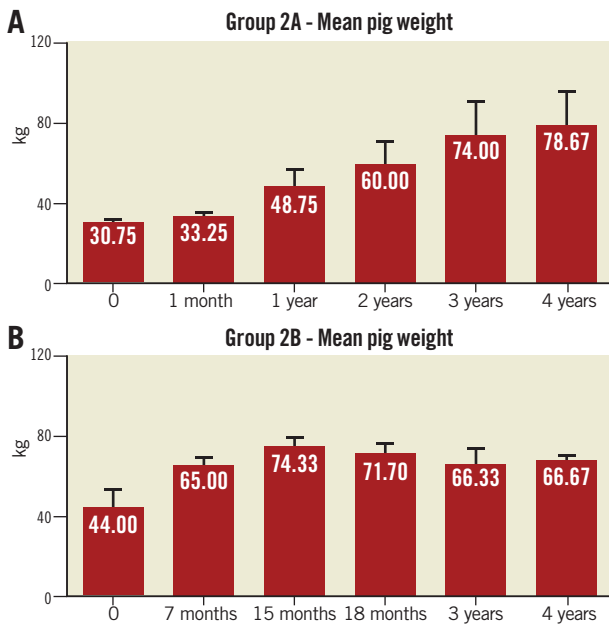


**Figure 5.** Animal weights at implantation and follow-up. A) Group 2A. B) Group 2B.

PLLA BRS was comparable to BMS in terms of safety, healing, biocompatibility and vessel patency. Importantly, the BRS elicited expansive vascular remodelling starting at one year, in the absence of antiproliferative drugs, which was probably related to progressive device dismantling and polymer resorption.

One of the major challenges of BRS is their limited mechanical strength and resistance to the compressive load imposed by the vessel following acute deployment in challenging anatomical conditions (i.e., severe calcification). In current-generation BRS, polymer orientation and crystallinity determine the mechanical strength of the scaffold. In turn, the polymer's ability to orient itself and gain

**Table 2.** Histologic evaluation of healing and inflammation at 28 and 90 days.

	BRS	BMS	p-value
<b>28 days</b>			
Peri-strut inflammation	0.55±1.16	0.03±0.10	0.563
Neointima inflammation	0.27±0.58	0.0±0.0	0.189
Endothelial coverage	4.0±0.0	4.0±0.0	1.000
Fibrin deposits	0.52±0.41	0.57±0.40	0.742
Adventitial fibrosis	0.51±0.67	0.84±0.70	0.339
<b>90 days</b>			
Peri-strut inflammation	1.25±1.30	0.11±0.16	0.530
Neointima inflammation	0.27±0.58	0.11±0.16	0.530
Endothelial coverage	4.0±0.0	4.0±0.0	1.000
Fibrin deposits	0.0±0.0	0.0±0.0	0.755
Adventitial fibrosis	0.84±0.73	0.28±0.30	0.731
All values expressed in this table are semiquantitative scores.			

crystallinity depends on its MW and the tube manufacturing process. The current-generation BRS technologies utilise low MW polymers because they can be readily oriented, allowing a substantial increase of their crystallinity. However, highly crystalline polymers cause the scaffolds to become more brittle, which significantly limits their resistance to fracture. This is the predominant reason why current-generation BRS are still limited by their capacity to overexpand beyond pre-determined limits and to resist vascular recoil under extreme conditions, even though they have otherwise achieved levels of biomechanical performance equivalent to metallic stents<sup>13-16</sup>. New-generation polymers using very high MW PLLA promise to improve the biomechanical properties of current-generation BRS by largely depending on the intrinsic material properties uniquely associated with the ultrahigh MW and proprietary manufacturing methodology instead of purely relying on polymer orientation and

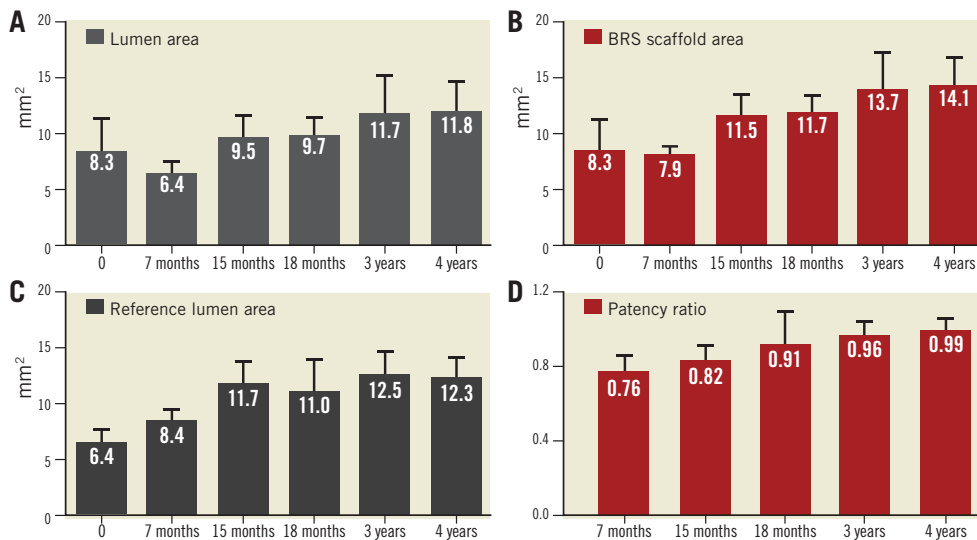


**Figure 6.** Long-term OCT follow-up of animals treated with BRS only (group 2B). Increases in lumen area (A), scaffold area (B), reference lumen area (C) and patency ratio (D) were demonstrated.

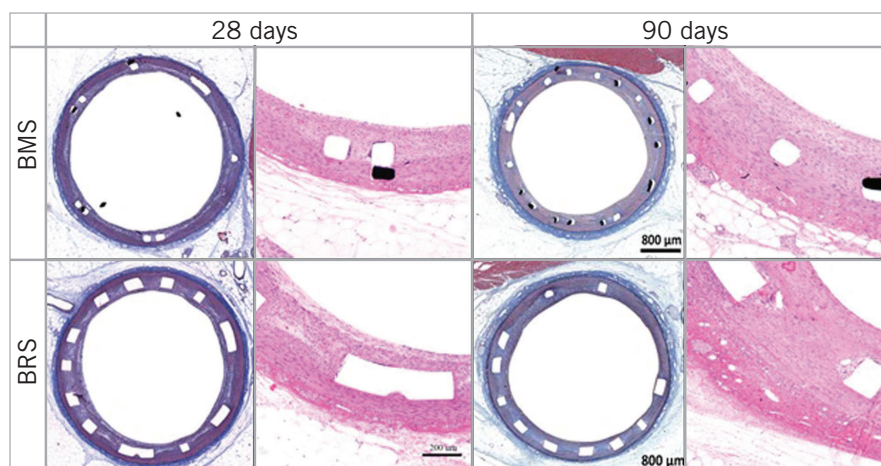


**Figure 7.** Histology images of animals implanted with BRS and BMS at 28 and 90 days.

crystallinity. *Ex vivo* studies show that this type of polymer dramatically improves overexpansion capabilities and resistance to fracture under static and dynamic conditions compared to clinically available BRS (Juan Granada, MD, unpublished data, 2016).

The optimal time course for the *in vivo* degradation of BRS remains a topic of an ongoing debate. Data from patients undergoing percutaneous transluminal coronary angioplasty (PTCA) suggest that scaffold support for the arterial wall is required for at least three to four months<sup>17,18</sup>. Experimental data using a poly-DL lactic acid drug-free BRS in a porcine model showed that a BRS displaying a rapid degradation profile (MW loss ~86% at six months) presented healing profiles similar to BMS at six months<sup>19</sup>. However, clinical data suggest that rapid polymer absorption reduces the radial force of the scaffold prematurely, which can lead to late recoil and adverse clinical events<sup>5,20</sup>. In the clinical setting, a longer resorption period (six to nine months) may provide a more stable device dismantling process and better clinical outcomes. The BRS tested in the present study is made of PLLA struts of 150 micron thickness that are arranged in a zigzag helical design with a peak circumferential radial force of ~0.11 MPa, similar to metallic stents right after deployment<sup>21</sup>. *Ex vivo* degradation and *in vivo* data demonstrated that the radial support is maintained for approximately eight to 10 months, at which time the MW was reduced by about 50%. Also, due to the particular polymer characteristics of the device tested, the radial force values displayed over time were maintained at a higher level compared to the Absorb™ BVS (Abbott Vascular, Santa Clara, CA, USA)<sup>22</sup>. This supports the fact that the tested scaffold provides radial support for a sufficient period of time to promote adequate healing and remodelling of the injured coronary segments.

An important objective of this study was to evaluate the impact of the polymer utilised in the FORTITUDE scaffold on vascular healing in the absence of antiproliferative drugs. The results are key because biocompatibility polymer data directly compared against metallic stents are not widely available in the BRS field. In this study, OCT imaging revealed that all BRS and BMS were well expanded, well positioned, and exhibited minimal recoil following implantation.

Neointimal proliferation, a surrogate marker of inflammation and healing, was comparable at each time point between BRS and BMS up to four years. Our histology results, although limited to 90 days, showed comparative healing indexes for both tested devices. The slightly increased %AS seen in the BRS group is probably the result of the thicker struts accommodating larger amounts of neointimal tissue compared to the thin-strut BMS. Also, the slightly higher levels of peri-strut inflammation seen in the BRS group at 90 days are probably related to the degradation process already underway. These differences, however, did not alter the overall healing profile observed in the BRS group over four years of follow-up.

We also studied the *in vivo* changes of the vessel architecture after implantation of the BRS in the absence of everolimus, which is important because the biological variables responsible for the process of expansive remodelling are still unknown. Our data demonstrate that the LA of the reference segments increased over time, reflecting normal growth of the animal. However, this occurred to a lesser degree in BMS-caged vessels than in the BRS-treated vessel segments. The lumen area declined at 90 days in the BMS group reflecting neointimal growth, followed by neointimal stabilisation resulting in slight lumen increase at two years. In BRS-treated segments, the LA also declined at the same time point due to early neointimal formation; however, we observed a steady increase in lumen gain over four years. Additionally, the reproducibility of our data was confirmed by the results from animals implanted only with BRS, which showed the same remodelling pattern. However, it is noteworthy that these experiments were performed in young adult Yucatan pigs. Therefore, the animals grew and gained weight in the first two years of follow-up. Consistent with this, we observed an increase in the coronary lumen area of the reference vessels during the early phase of follow-up. In contrast, after the second year of follow-up, the reference lumen area was very stable, indicating no further vessel growth. Importantly, the patency ratio of the BRS-treated vessels increased over time and reached a ratio of one after four years of follow-up. This demonstrates that the BRS accommodated the natural growth of the vessels. In contrast, the patency

ratio of the BMS-treated vessels decreased over the first two years and then plateaued because the stented segment did not match the growth of the reference segment. Moreover, the BRS-treated segments demonstrated evidence of expansive vascular remodelling because the BRS lumen area exceeded the reference lumen area after two years. The degree of expansive vascular remodelling seen in our study is consistent with that observed with other BRS in porcine models, and correlates with the MW loss occurring over time<sup>23</sup>. In addition, qualitative OCT analysis showed a progressive decrease in the number and size of black cores between one and four years following scaffold implantation. However, a small percentage of black core-like structures was still identified at this time point. It has been suggested that the presence of black core-like structures does not necessarily correlate with the presence of residual polymer in humans in the Absorb BVS up to four-year follow-up<sup>24</sup>. Unfortunately, at the present time, whether these black cores reflect the residual polymer presence is still unknown, as the four-year OCT histological data correlation analysis is still under development.

Our study contributes to the BRS literature as it introduces a novel polymeric device concept and has tested its biocompatibility against a clinically available BMS control in the absence of antiproliferative drugs. The long-term biocompatibility of fully bioresorbable scaffolds in the absence of limus analogues was previously believed to be inferior to BMS platforms. Our data also support some of the biological findings of a previous report by our group that employed a different non-drug-eluting BRS<sup>23</sup>. Together, these results indicate that the biological effects of BRS on late lumen gain and vascular restoration<sup>6</sup> are independent of antiproliferative drugs, and this appears to be a class effect. Our findings also validate the biomechanical properties and biocompatibility of this ultrahigh MW amorphous PLLA polymer in the absence of antiproliferative drugs. These findings are relevant as the two-year follow-up of the first-in-human clinical study using this device has been completed, confirming the biocompatibility and biomechanical properties of this device in humans. Also, enrolment to the first-in-human study using the same PLLA sirolimus-eluting BRS platform has already been completed (Juan Granada, MD, unpublished data, 2016).

## Limitations

The present study has some limitations worth highlighting. First, the performance of the novel BRS was examined in healthy coronary arteries in a swine model of restenosis. Therefore, although our data support the safety and biocompatibility of the device, our findings cannot predict clinical performance among patients with a high atherosclerotic burden. Second, our study included only 28- and 90-day histological data. The reported study is part of a large five-year biocompatibility study, and therefore all the animals are still undergoing imaging follow-up. The 28- and 90-day interim data provide a snapshot of the healing profile, but long-term histological data are not yet available. However, we believe that the imaging findings are appropriate surrogates for the evaluation of healing and, in view of the positive long-term imaging

results, long-term histological data will probably not change the conclusions of the present study.

## Conclusions

In conclusion, our results indicate that the BRS utilised in the present study was comparable to a control BMS in terms of biocompatibility and vascular healing at four years in healthy porcine arteries. In contrast to the arterial segments treated with the BMS, the BRS-treated arterial segments underwent expansive remodelling in parallel with the degradation process of the polymer scaffold. These findings suggest that the ultrahigh MW amorphous PLLA formulation assessed in this study has the potential to improve the performance of current-generation BRS by providing a highly biocompatible and mechanically durable platform at lower strut thickness levels.

## Impact on daily practice

The non-drug-eluting BRS used in the present study (FORTITUDE) was comparable to the control BMS in terms of safety, biocompatibility and efficacy in maintaining coronary arterial patency. Interestingly, the BRS-treated arterial segments demonstrated evidence of positive remodelling and late lumen gain even in the absence of antiproliferative drug elution. The BRS used in this study is currently under investigation in first-in-human studies, and therefore preclinical testing of the safety and biocompatibility profile is of clinical importance.

## Funding

This study was funded by Amaranth Medical, Inc., Mountain View, CA, USA.

## Conflict of interest statement

At the time the study was performed, the authors K. Ramzipoor, C. Lee and E. Estrada were full-time employees of Amaranth Medical, Inc. The other authors have no conflicts of interest to declare.

## References

1. Ormiston JA, Serruys PW, Regar E, Dudek D, Thuesen L, Webster MW, Onuma Y, Garcia-Garcia HM, McGreevy R, Veldhof S. A bioabsorbable everolimus-eluting coronary stent system for patients with single de-novo coronary artery lesions (ABSORB): a prospective open-label trial. *Lancet*. 2008;371:899-907.
2. Serruys PW, Onuma Y, Dudek D, Smits PC, Koolen J, Chevalier B, de Bruyne B, Thuesen L, McClean D, van Geuns RJ, Windecker S, Whitbourn R, Meredith I, Dorange C, Veldhof S, Hebert KM, Sudhir K, Garcia-Garcia HM, Ormiston JA. Evaluation of the second generation of a bioresorbable everolimus-eluting vascular scaffold for the treatment of de novo coronary artery stenosis: 12-month clinical and imaging outcomes. *J Am Coll Cardiol*. 2011;58:1578-88.
3. Onuma Y, Serruys PW, Gomez J, de Bruyne B, Dudek D, Thuesen L, Smits P, Chevalier B, McClean D, Koolen J, Windecker S,



- Whitbourn R, Meredith I, Garcia-Garcia H, Ormiston JA; ABSORB Cohort A and B investigators. Comparison of in vivo acute stent recoil between the bioresorbable everolimus-eluting coronary scaffolds (revision 1.0 and 1.1) and the metallic everolimus-eluting stent. *Catheter Cardiovasc Interv.* 2011;78:3-12.
4. Wu Y, Shen L, Wang Q, Ge L, Xie J, Hu X, Sun A, Qian J, Ge J. Comparison of acute recoil between bioabsorbable poly-L-lactic acid XINSORB stent and metallic stent in porcine model. *J Biomed Biotechnol.* 2012;2012:413956.
  5. Ormiston JA, Serruys PW, Onuma Y, van Geuns RJ, de Bruyne B, Dudek D, Thuesen L, Smits PC, Chevalier B, McClean D, Koolen J, Windecker S, Whitbourn R, Meredith I, Dorange C, Veldhof S, Hebert KM, Rapoza R, Garcia-Garcia HM. First serial assessment at 6 months and 2 years of the second generation of absorb everolimus-eluting bioresorbable vascular scaffold: a multi-imaging modality study. *Circ Cardiovasc Interv.* 2012;5:620-32.
  6. Lane JP, Perkins LE, Sheehy AJ, Pacheco EJ, Frie MP, Lambert BJ, Rapoza RJ, Virmani R. Lumen gain and restoration of pulsatility after implantation of a bioresorbable vascular scaffold in porcine coronary arteries. *JACC Cardiovasc Interv.* 2014;7:688-95.
  7. Serruys PW, Garcia-Garcia HM, Onuma Y. From metallic cages to transient bioresorbable scaffolds: change in paradigm of coronary revascularization in the upcoming decade? *Eur Heart J.* 2012;33:16-25b.
  8. Okamura T, Garg S, Gutierrez-Chico JL, Shin ES, Onuma Y, Garcia-Garcia HM, Rapoza RJ, Sudhir K, Regar E, Serruys PW. In vivo evaluation of stent strut distribution patterns in the bioabsorbable everolimus-eluting device: an OCT ad hoc analysis of the revision 1.0 and revision 1.1 stent design in the ABSORB clinical trial. *EuroIntervention.* 2010;5:932-8.
  9. Otsuka F, Pacheco E, Perkins LE, Lane JP, Wang Q, Kamberi M, Frie M, Wang J, Sakakura K, Yahagi K, Ladich E, Rapoza RJ, Kolodgie FD, Virmani R. Long-term safety of an everolimus-eluting bioresorbable vascular scaffold and the cobalt-chromium XIENCE V stent in a porcine coronary artery model. *Circ Cardiovasc Interv.* 2014;7:330-42.
  10. Serruys PW, Chevalier B, Dudek D, Cequier A, Carrié D, Iniguez A, Dominici M, van der Schaaf RJ, Haude M, Wasungu L, Veldhof S, Peng L, Staehr P, Grundeken MJ, Ishibashi Y, Garcia-Garcia HM, Onuma Y. A bioresorbable everolimus-eluting scaffold versus a metallic everolimus-eluting stent for ischaemic heart disease caused by de-novo native coronary artery lesions (ABSORB II): an interim 1-year analysis of clinical and procedural secondary outcomes from a randomised controlled trial. *Lancet.* 2015;385:43-54.
  11. Dudek D, Rzeszutko Ł, Zasada W, Depukat R, Siudak Z, Ochała A, Wojakowski W, Przewłocki T, Żmudka K, Kochman J, Lekston A, Gąsior M. Bioresorbable vascular scaffolds in patients with acute coronary syndromes: the POLAR ACS study. *Pol Arch Med Wewn.* 2014;124:669-77.
  12. Ellis SG, Kereiakes DJ, Metzger DC, Caputo RP, Rizik DG, Teirstein PS, Litt MR, Kini A, Kabour A, Marx SO, Popma JJ, McGreevy R, Zhang Z, Simonton C, Stone GW; ABSORB III Investigators. Everolimus-Eluting Bioresorbable Scaffolds for Coronary Artery Disease. *N Engl J Med.* 2015;373:1905-15.
  13. Ormiston JA, De Vroey F, Serruys PW, Webster MW. Bioresorbable polymeric vascular scaffolds: a cautionary tale. *Circ Cardiovasc Interv.* 2011;4:535-8.
  14. Stankovic G, Darremont O, Ferenc M, Hildick-Smith D, Louvard Y, Albiero R, Pan M, Lassen J, Lefèvre T; European Bifurcation Club. Percutaneous coronary intervention for bifurcation lesions: 2008 consensus document from the fourth meeting of the European Bifurcation Club. *EuroIntervention.* 2009;5:39-49.
  15. Foin N, Lee R, Mattesini A, Caiazzo G, Fabris E, Kilic D, Chan JN, Huang Y, Venkatraman SS, Di Mario C, Wong P, Nef H. Bioabsorbable vascular scaffold overexpansion: insights from in vitro post-expansion experiments. *EuroIntervention.* 2016;11:1389-99.
  16. Džavík V, Colombo A. The absorb bioresorbable vascular scaffold in coronary bifurcations: insights from bench testing. *JACC Cardiovasc Interv.* 2014;7:81-8.
  17. Nobuyoshi M, Kimura T, Nosaka H, Mioka S, Ueno K, Yokoi H, Hamasaki N, Horiuchi H, Ohishi H. Restenosis after successful percutaneous transluminal coronary angioplasty: serial angiographic follow-up of 229 patients. *J Am Coll Cardiol.* 1988;12:616-23.
  18. Serruys PW, Luijten HE, Beatt KJ, Geuskens R, de Feyter PJ, van den Brand M, Reiber JH, ten Katen HJ, van Es GA, Hugenholtz PG. Incidence of restenosis after successful coronary angioplasty: a time-related phenomenon. A quantitative angiographic study in 342 consecutive patients at 1, 2, 3, and 4 months. *Circulation.* 1988;77:361-71.
  19. Durand E, Sharkawi T, Leclerc G, Raveleau M, van der Leest M, Vert M, Lafont A. Head-to-head comparison of a drug-free early programmed dismantling polylactic acid bioresorbable scaffold and a metallic stent in the porcine coronary artery: six-month angiography and optical coherence tomographic follow-up study. *Circ Cardiovasc Interv.* 2014;7:70-9.
  20. Tanimoto S, Bruining N, van Domburg RT, Rotger D, Radeva P, Ligthart JM, Serruys PW. Late stent recoil of the bioabsorbable everolimus-eluting coronary stent and its relationship with plaque morphology. *J Am Coll Cardiol.* 2008;52:1616-20.
  21. Oberhauser JP, Hossainy S, Rapoza RJ. Design principles and performance of bioresorbable polymeric vascular scaffolds. *EuroIntervention.* 2009;5 Suppl F:F15-22.
  22. Onuma Y, Serruys PW. Bioresorbable scaffold: the advent of a new era in percutaneous coronary and peripheral revascularization? *Circulation.* 2011;123:779-97.
  23. Strandberg E, Zeltinger J, Schulz DG, Kaluza GL. Late positive remodeling and late lumen gain contribute to vascular restoration by a non-drug eluting bioresorbable scaffold: a four-year intravascular ultrasound study in normal porcine coronary arteries. *Circ Cardiovasc Interv.* 2012;5:39-46.
  24. Stone GW, Granada JF. Very Late Thrombosis After Bioresorbable Scaffolds: Cause for Concern? *J Am Coll Cardiol.* 2015;66:1915-7.